Chemical Engineering Journal 162 (2010) 415–423

Contents lists available at ScienceDirect

Chemical Engineering Journal

journal homepage: www.elsevier.com/locate/cej

Optimization of process parameters on the extrusion of honeycomb shaped monolith of H-ZSM-5 zeolite

A. Aranzabal*, D. Iturbe, M. Romero-Sáez, M.P. González-Marcos, J.R. González-Velasco, J.A. González-Marcos

Group "Chemical Technologies for Environmental Sustainability", Chemical Engineering Dept, Faculty of Sciences and Technology, Universidad del País Vasco/EHU, P.O. Box 644, E-48080 Bilbao, Spain

ARTICLE INFO

Article history:
Received 21 January 2010
Received in revised form 11 May 2010
Accepted 20 May 2010

Keywords:
Monolith
Zeolite
H-ZSM-5
Binder
Extrusion
Process optimization
Catalytic reactions

ABSTRACT

The optimization of the process parameters for the preparation of H-ZSM-5 zeolite monolith structure by direct extrusion technique is reported. This preparation method avoids the difficulties associated with the anchoring the crystalline zeolite material to the monolithic support or with the uniform synthesis of zeolite along the whole monolith, and shows the advantage that the active phase is uniformly distributed throughout the monolith and reduces the number of steps necessary for the preparation: paste preparation, extrusion, drying and firing. Colloidal silica was used as a permanent binder and methylcellulose as a temporary binder. It was found the best paste composition (zeolite, binders and water) to assure best rheological properties must show stabilized drive torque around 10 N m in wet kneading. Extrusion through high quality designed nozzle (123 cells/in.^{2}) resulted optimal at conditions of room temperature and the highest extrusion-rate without formation of surface defects (40 rpm). Drying of the green monoliths at heating rates lower than 0.15 °C min^{-1} in the initial stages prevents from the migration of the binder and led to a uniform shrinkage avoiding formation of fractures or deformities. Resulted monoliths showed high activity in the oxidation of chlorinated volatile organic compounds.

1. Introduction

During the last decades, zeolites have gained interest as potential active catalysts for the abatement of atmospheric pollutants in the flue-gases, e.g. oxidation of volatile organic compounds (VOC) and selective reduction of NO_x [1], because of their pore structures, acidic properties, good thermal stability and ion exchange properties. Most of the studies have been performed in fixed bed laboratory reactors using powder catalysts. However, the scale up of the process using powder catalyst is no recommended because of the high pressure drop associated with the high flow rates to be treated. Therefore, for practical environmental applications, these catalysts should be shaped as honeycomb monoliths, enabling low pressure drop and good tolerance to plugging by dust [2].

Preparation technologies of monolithic catalysts have been reviewed several times [3–7]. Summing up, the most common method to prepare monolith structures based on zeolites, as the catalytically active material, is by coating with a thin film of zeolite on the external walls of an inert ceramic monolith substrate. Cordierite is the preferred material for monolithic structures because of its high mechanical strength and its low thermal expansion coefficient [8]. The usual coating techniques are dip-coating, slip-coating and slurry coating [9], but more recently in situ zeolite synthesis techniques have been successfully developed [10,11]. The advantages of this type of catalyst are those associated to the strength of the cordierite and to the low consumption of the active material. Disadvantages are associated firstly, with the anchoring problems of crystalline zeolite materials, and secondly, with the difficulties to uniform synthesis of zeolite along the whole monolithic substrate.

An alternative method to introduce the active phase in a monolith is by direct extrusion of the catalytic material, as zeolites. Thus, the active phase is distributed throughout the monolith and also significantly reduces the number of steps necessary for the preparation. Papers reporting extrusion of zeolite monolith in the literature is limited to zeolite A [12–15], but there is very little data about extrusion of other type of zeolites (mordenite, ZSM-5, Beta, etc.) [7].

Monoliths of ceramic materials are manufactured following the same steps outlined for cordierite [16] and zeolite A [13] extrusion, but using the corresponding raw material. The basic steps are: (1) dry mixing of the solid materials (oxides or salts and binders); (2) wet mixing and kneading (water and additives: organic and/or inorganic); (3) extrusion of the paste thorough special dies to form the monolithic honeycomb shape; (4) drying uniformly; (5) firing. Each of these steps is function of one or more of variables. The rheological properties of the paste are critical to extrude a defect-free honeycomb shaped monolith [16]. Getting good rheological properties

* Corresponding author. Tel.: +34 946015554; fax: +34 946013500.
E-mail address: asier.aranzabal@ehu.es (A. Aranzabal).

1385-8947/$ – see front matter © 2010 Elsevier B.V. All rights reserved.
doi:10.1016/j.cej.2010.05.043

Table 1
Specifications of raw materials.

NH_4-ZSM5 zeolite powder	
Chemical formula	$NH_4^+{}_n\ (H_2O)_{16}[Al_nSi_{96-n}\ O_{192}]$, $n<27$
Product reference	CBV5524G (Zeolyst)
SiO_2/Al_2O_3 ratio	50
Na_2O	0.05%
Surface area	425 $m^2\ g^{-1}$
Methyl cellulose	
Chemical formula	$[C_5O(OCH_3)_4OC_5O(OCH_3)_3]_nCH_3$
Product reference	M0512 (Merck)
Viscosity	4.000 MPa s, 2% in H_2O (20 °C)
Molecular weight	80,000 g mol^{-1}
Colloidal silica	
Chemical formula	SiO_2
Product reference	LUDOX® HS-40 colloidal silica (Aldrich)
Concentration	40 wt.% suspension in H_2O
Molecular weight	60.08
Surface area	~220 m^2/g
pH	9.8
Density	1300 kg m^{-3} at 25 °C

depends on the paste composition, kneading speed and temperature, as well as, extrusion speed and temperature. This is the most difficult task since each variable affect directly to the quality of the final product. The combination of heating and dehumidification rates is also critical in the drying and firing steps in order to avoid formation of cracks and to provide the monolith with high mechanical strength. Then, the objective of this work is find out the best combination of process parameters to produce a strong honeycomb shaped monolith of H-ZSM-5 for off-gases purification. ZSM-5 zeolite was chosen for monolith fabrication as a potential catalyst for the oxidation of chlorinated VOC [17].

For zeolitic materials high values of surface areas, 200–400 m g^{-1}, are achievable, but the mechanical strength is significantly lower than those of low-surface area monoliths (cordierite). Then, it is necessary to include permanent binders to increase its mechanical strength. Its composition is usually similar to that of the main material of the monolith, so as to not modify its catalytic properties. Perera and co-workers [13,14] used bentonite as a binder a firing temperature of 800 °C to sinter the binder and enhance the strength of the monolith, for 5A zeolite monoliths. Grande et al. [12] used methyl siloxane ether, which was transformed in SiO_2 at 650 °C. Shams and Mirmohammadi [15] fired their 5A zeolite mixed with kaolin to transform into metakaolin. In general terms, it is necessary to adopt a compromise solution in the heat treatment temperature to achieve an elevated mechanical stability without loosing catalytic properties of the zeolite. Preliminary works carried out in our laboratories in order to select the binder composition that provides a high mechanical strength without reducing catalytic properties of the zeolite had led us to choose the colloidal silica as the best permanent binder [18].

2. Experimental

The zeolite powder NH_4-ZSM-5 was supplied by the Zeolyst Corp., and was used as received. Synthetic methylcellulose polymer (M-0512) used as organic temporary binder, was supplied by Sigma Chemical Co. SiO_2 was used as colloidal suspension in water of discrete uniform spheres of silica. The commercial name of this product is Ludox® HS-40, and it was supplied by Aldrich. Table 1 shows the specifications of the raw material.

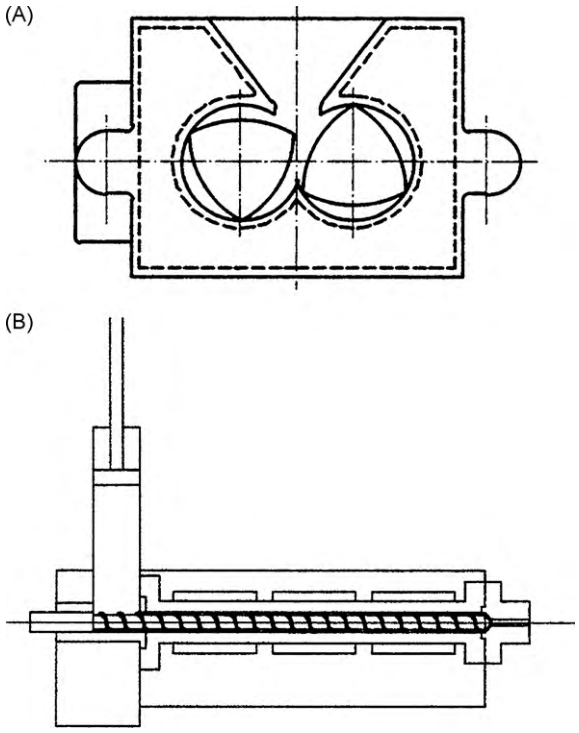

Fig. 1. (A) Cross section of the mixing head. (B) Cross section of extrusion head.

2.1. Preparation of extrudates

For preparation of zeolite type and honeycomb shape extrudates a DATA PROCESSING PLASTI-CORDER® PL-2000 computerized torque rheometer system has been used. The interchangeable BRABENDER® measuring heads allow testing processes of mixing, kneading and extruding.

Mixing and kneading process was carried out in a BRABENDER® laboratory 350-E mixer head, equipped with two mixing blades, one turning faster than the other (Fig. 1). The force or torque required to keep the blades turning at a constant speed is measured, and the temperature is monitored by a thermocouple protruding through the bowl into the mixer. It also can be heated up with either 1 or 2 separate control circuits. The temperature control has been done by a Grant LTD20 thermostatic bath with liquid (ethylene glycol–water mixture) circulation in the range of −30 and 100 °C.

Precursor ceramic paste was extruded by 19/20DN BRABENDER® extrusion head mounted onto the base plate of PLASTI-CORDER® PL-2000 (Fig. 1). The extruder barrel with 19 mm screw diameter and a length of 20 D was heated/cooled in three sections by means of thermostatic liquid circulation described before. The barrel has 8 threaded bores (Dynisco bores) altogether opposite to each other to hold pressure transducers and thermocouples for measuring melt pressure and melt temperature. For feeding ceramic paste, a pneumatic loading chute perpendicular to barrel is used.

For honeycomb shape monolith production, self-designed die head with circular (Fig. 2) geometry and density of 123 cells/in.^{2}, was mounted into the die head.

2.2. Characterization of monolith zeolites

The BET surface areas and pore volumes of the zeolite samples were determined by N_2 adsorption–desorption at −196 °C in a Micromeritics ASAP 2010 equipment.

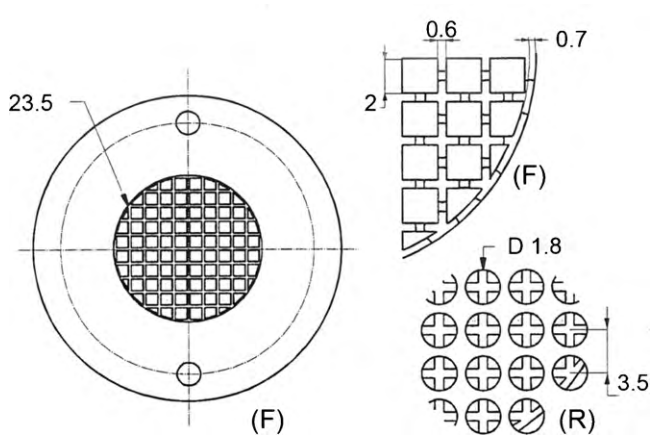

Fig. 2. Self-designed extrusion nozzle of circular shaped with 123 cells/in.^{2}. (F) Front view; (R) rear view.

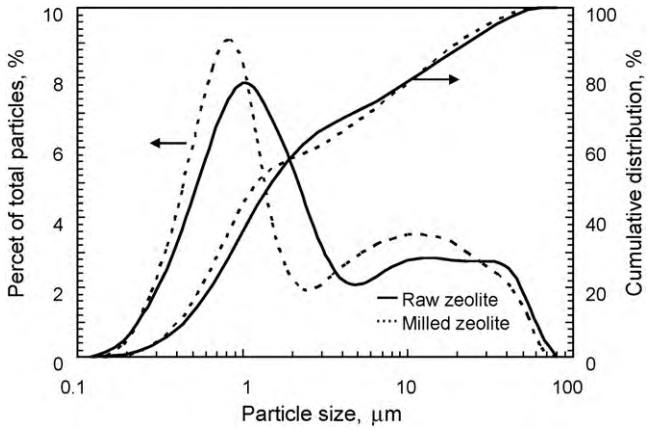

Fig. 3. Particle size distribution of zeolites.

Temperature-programmed desorption (TPD) of ammonia was performed on a Micromeritics AutoChem 2910 instrument. Prior to adsorption experiments, the samples (30–40 mg) were first pretreated in a quartz U-tube in a nitrogen stream at 500 °C. Then, they were cooled down at 100 °C in a N_2 flow (20 $cm^3\ min^{-1}$) before the ammonia adsorption started. The adsorption step was performed by admitting small pulses of ammonia in Ar at 100 °C up to saturation. Subsequently, the samples were exposed to a flow of argon (50 $cm^3\ min^{-1}$) for 2 h at 100 °C in order to remove reversibly and physically bound ammonia from the surface. Finally, the desorption was carried out from 100 to 500 °C at a heating rate of 10 °C per min in an Ar stream (50 $cm^3\ min^{-1}$). This temperature was maintained for 15 min until the adsorbate was completely desorbed.

The particle size distribution was determined by laser scattering in a Malvern Mastersizer equipment.

The X-ray powder diffraction (XRD) patterns for the measurement of the zeolite crystallinity, were recorded on a Philips PW 1710 X-ray diffractometer with Cu Kα radiation and Ni filter.

The surface topology of zeolite powder and monolith was compared by Scanning Electron Microscope (SEM) in a JEOL JSM-6400 instrument. The monoliths were carefully cut in parallel and perpendicular cuts to the monolith axis.

The mechanical strength of the extruded materials was evaluated with a MMT-100 Metrotec multitest dynamometer. Cylindrical probes of 21 mm diameter and 21 mm length were extruded and subjected to a axial constant loading rate of 1.3 mm min^{-1} until it was crushed, according to ASTM C133-97 standard.

The catalytic activity of the monoliths was measured in the experimental set-up described elsewhere [17]. A new reactor was made with a specific diameter to house tightly inside the monolith. The reactions were carried out by feeding $1.33 \times 10^{-5}\ m^3 N\ s^{-1}$ of air and 5.9×10^{-7} mol s^{-1} (1000 ppmv) of 1,2-dichloroethane (DCE) and placing 3.38×10^{-3} kg of catalyst. The temperature was varied progressively increasing from 200 to 450 °C as conversion of DCE was measured.

3. Results and discussion

3.1. Particle size of raw materials

Particle size and distribution of the raw materials plays an important role in the ceramic support preparation, not only in the washcoating technology [19] but also in the extrusion process, since the rheological properties (and therefore fluidicity) are function of them [20]. It is very important that particle size distribution of zeolite crystals being small and broadly enough in order to get stronger packing between particles and large enough with respect to the particles of binder, so that the binding is most effective, as stated above. As reported by Robinson [21], non-plastic particles larger than 600 μm encourage tearing, drying cracks and transverse lamination cracking. Particle sizes of non-plastics between 600 and 150 μm will break up large lamination cracks into many small cracks. A combination of these particles with 125 μm non-plastics are more effective than an equal quantity of larger-size particles in reducing plasticity and cohesion and working towards elimination of surface cracking.

Zeolite and silica are considered as non-plastic. As shown in Fig. 3, ZSM-5 zeolite shows a broad distribution (0.1–80 μm), with two peaks at 1 and 15 μm, respectively. It seemed to be adequate for paste preparations, because of the relatively small size and wide range. In order to analyze the influence of the zeolite particle size in the extrusion process, raw zeolite was milled (with zirconia balls in a Retsch mill) up to 60 min. Though particle size was slightly reduced (Fig. 3), the change was too little so as to affect to the extrusion process, as reported by Ferret [22]. Then, raw zeolite was used for all the experiments.

Colloidal silica binder's particle size is about 11.5 nm as reported by the supplier, which is also adequate, as they are some orders of magnitude smaller with respect to zeolite powder. Then, the particle size distribution of these materials is broad enough to achieve good filling of inter-particle hollows.

3.2. Optimization of the kneading stage

The first stage in forming ceramic extrudates is to prepare the paste to be extruded. The paste is composed with the solid powders selected for the chemical composition of the final product (zeolite and binder) with the proper amount of liquid and/or other additives (synthetic methylcellulose polymer temporary binder) in such a way, the resulting material can be readily extruded and moulded [16,23]. The optimization of this step consists on selecting the best paste composition and operating conditions (temperature and blades' speed) to provide the paste with best rheological properties (elasticity, plasticity and viscosity) for extrusion. Mixing and kneading consist on three processing stages: dry mixing, wet kneading and high-shear mixing [16].

3.2.1. Dry mixing

Dry mixing should ideally yield a uniform distribution of all of the solid components. The dry mixing stage is a necessary precursor to paste formation and must be selected with care. Although it is preferred binders to be added as solid powder [4], as SiO_2 binder

Table 2
Optimized dry-mixing conditions.

Total mass of solids, g	144–155
NH_4-ZSM5, %	92–96
Methylcellulose, %	4–8
Temperature, °C	17
Speed, rpm	40
Time, min	20

is supplied as a 40% colloidal suspension in water, it will be added in the wet mixing stage. Then, zeolite powder and methylcellulose polymer were mixed in a BRABENDER® laboratory 350-E mixer head as described above.

Dry mixing experiments where carried out by changing total amount of mass and rotation speed of blades and by monitoring torque, in order to select the conditions that make it a vigorous mixing without splitting mass out. Though its total volume was 390 cm^3, it should not be filled up more than 80%, because of the heat generated during mixing and the expansion of the paste when water was added. But it must to be filled up enough to prevent from mixing-shortcuts, resulting in non-homogenous mixing.

By visual observation of mixing quality, conditions of room temperature and 40 rpm speed of blades were selected. Dry mixing time was fixed to 20 min, since torque reached a stationary value (uniform mixing) at 15 min. Table 2 shows selected dry-mixing conditions.

3.2.2. Wet kneading

The wet kneading was also carried out in the same laboratory 350-E Brabender mixer. Once the solid mixture was homogeneous (20 min), immediately SiO_2 colloidal suspension (permanent binder) and water were successively added. A quantity of liquid sufficient to fill the voids between the powder particles ensures that high green densities are achieved and therefore high mechanical strength of the green monolith [24]. The optimization of liquid content is very important, since it has been concluded that just small quantities of excess liquid increase the ease of extrusion, but seepage also can happen. On the contrary loss of a little liquid produces a drastic rise in flow resistance and the paste becomes stiff and even in some instances impossible to extrude [25]. Lamination defects observed during calcination of extruded material with high water content shows there is direct correlation between water content on the green ceramic paste and morphological and mechanical properties in the final product [21].

The appropriate degree of plasticity and consistency of the paste is related with the stationary drive torque applied during wet kneading process to keep constant the rotational speed of the blades. This value of torque is related with the mass of materials and the configuration of the mixer. In this step a set of experiments were carried out by changing water, methylcellulose and SiO_2 content, temperature and rotation speed of blades, in order to select the composition and kneading conditions to produce extrudable zeolite based paste.

Fig. 4 shows the profile of the drive torque during kneading process for pastes with different water content. By the addition of water quick increase of the drive torque is observed, followed by gradual decrease until stationary value is reached. As methylcellulose polymer his hydrated, it is inflated. Then, it increases viscosity and changes flow characteristics to pseudo plastic. The time-average volume of the binder molecule is distorted by shear forces in the liquid, and the molecules tend to line up in a manner to reduce the resistance to flow [26].

It can be observed (Fig. 4) that as the water content is lower the drive torque sudden increase happens later, i.e. for 40% water (*with respect to total solid content*) it lasted 40 min for overall hydration of methylcellulose. The stationary drive torque falls down to

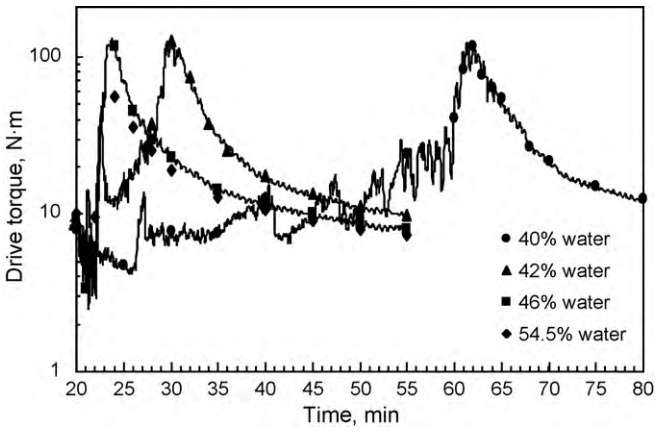

Fig. 4. Drive torque evolution during wet-keading of ZSM-5 for different water content. Solid phase composition: 3% methylcellulose, 17% SiO_2, 80% NH_4-ZSM-5.

12 N m. In this case the resulting green paste is too dry and with low plasticity. Increasing water content to 42%, stationary drive torque decreases to 10 N m. The resulting paste is less dry but still not plastic enough. Pastes with 46 and 54.5% water resulted too wet because the extrudate collapsed after it left the extruder. In both cases, stationary drive torque decreases to 8 N m. Then we conclude the optimum water content is around 42%, but it requires higher methylcellulose content in increase plasticity.

The time for wet-kneading step was established to 35 min, as the time for drive torque to stabilize after sudden increase.

The increase viscosity and change flow characteristics to pseudo plastic during wet kneading causes also temperature increase up to 40 °C, resulting in partial evaporation of water. Then 17 °C was set to as optimum temperature, since it increased only 4 °C during high torque application, before initial value is restored. At this temperature the viscosity and cohesive strength of the mix increased and it lost its adhesive character, thereby permitting good mould release and integrity for ejection.

The rotation speed of 40 rpm was also applied as in the dry mixing step, since good mixture between water and solid was observed.

Fig. 5 shows the profile of the drive torque during kneading process for ZMS-5 zeolite with different methylcellulose content. Stationary drive torque was 10 N m for the 3 and 5% compositions. However, 5% methylcellulose paste showed better plasticity and less sticky, then more easy to manipulate. 7% composition paste showed similar properties as the 5% one.

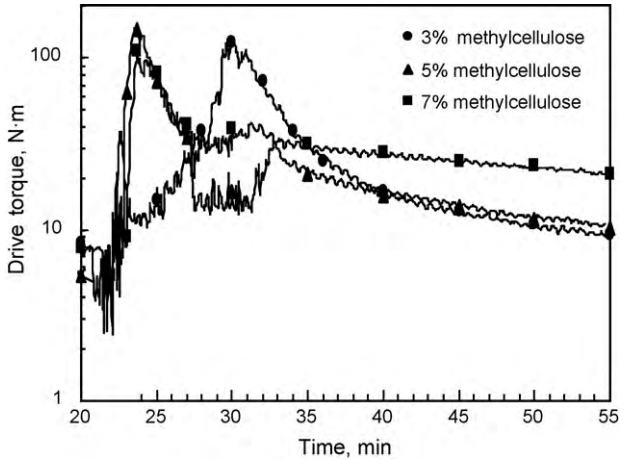

Fig. 5. Drive torque evolution during wet-keading of ZSM-5 for different methylcellulose content and 17% SiO_2 of solid phase. Water content is 42% with respect to total solid content.

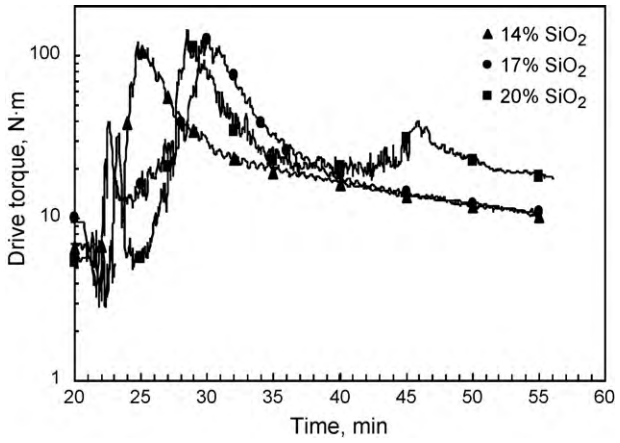

Fig. 6. Drive torque evolution during wet-keading of ZSM-5 for different SiO_2 and 3% of methylcellulose content in solid phase. Water content is 42% with respect to total solid content.

Fig. 6 shows the effect of SiO_2 permanent binder in the kneading process. The paste of ZSM-5 with 20% SiO_2 (18 N m stationary drive torque), was not plastic at all, and too hard as to manipulate. However, there was no difference between 14 and 17% SiO_2 pastes. Both resulted in high plasticity and cohesivity. Then, 14% composition was selected so as to reduce raw material consumption.

Monitoring the drive torque while wet kneading we concluded that the appropriate degree of plasticity in the paste is related with the stationary drive torque. The optimum value is within a narrow range around 10 N m. If it is higher the paste is too viscous and will not be able to cross the extrusion die and if it is lower the green monoliths will collapse. The selected kneading conditions are summed up in Table 3.

3.2.3. High-shear mixing

High-shear mixing is required in some applications in order to break down the agglomerates inherent in the starting powder and those formed during mixing. It is desirable to ensure the creation of single particles with a liquid layer or film covering the whole surface of each particle. In this process it is important that the liquid viscosity be high so that liquid seepage does not happen [16], and to prevent the creation of voids in the structure during extrusion stage. It also allows the paste to increase density by compacting, which will allow applying higher pressure for extrusion.

This stage is especially important when kneading is carried out in mixers with blades, in which static zones can emerge [24]. Among available techniques for high-shear mixing, based in our previous experience [22] kneading at low rotation speed of blades, has been chosen. As a blade is turned faster than the other, the paste is force to go through the space between them. The low shear rate make the paste to increase viscosity and compacting, as concluded in previous rheology studies [22]. This process was lasted the time enough to stabilize the monitored drive torque, which resulted in 15 min.

Table 3
Selected wet kneading conditions resulted from optimization research (the solid particle in the colloidal suspension of SiO_2, has been included within solid phase).

Solid phase mass, g	190
Zeolite, %	81
Methylcellulose, %	5
SiO_2, %	14
Liquid (water) mass, g	80
Temperature, °C	15–19
Rotational speed, rpm	40
Processing time, min	35

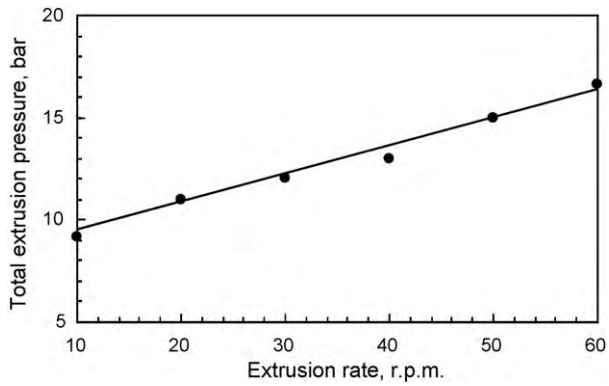

Fig. 7. Relation between total pressure applied in the extrusion and the extrusion rate, for the ZSM-5 zeolitic paste of Table 3.

The final green ceramic paste was keep in a environmental chamber at 15 °C and 85% relative humidity, during extrusion head mounting, so as to prevent paste aging by water migration to bulk surface.

3.3. Optimization of the extrusion stage

The key factors to obtain a high quality extrudate are a good design of the die head and control of the paste plasticity during extrusion. Assuming the die head is high quality designed, the optimization of the extrusion stage requires finding the extrusion conditions, i.e. extrusion temperature and rate that produces good honeycomb shape monolithic extrudates.

Due to viscous effects that occur in the extrusion through the nozzle, an excessive increase of temperature causes evaporation of water leading to a drier paste impossible to extrude. Conversely, cooling the extrusion process to an optimum temperature will favour the plastic behaviour of the paste by keeping its wet strength is at its maximum, and avoiding surface defects during extrusion. A set of experiments changing extrusion temperature from 19 to 45 °C, showed that the extrusion barrel must be cooled so as to kept temperature around 19–20 °C.

The extrusion rate influences on the presence of defects in the extrudate. Increasing extrusion rate, mass distribution is more uniform, which facilitates handing and avoids binder segregation during drying process. Conversely low extrusion rates led to voids formation in the green extrudate.

Determining the optimum extrusion rate, in order to avoid formation of surface defects, requires to perform experiments by recording extrusion pressure vs. extrusion rate, as the screw barrel rate. For materials behave as Bingham plastic, like zeolitic paste, higher initial force is required to start flowing. To achieve an accurate control of the extrusion and minimize the surface defects, the relationship between total pressure and extrusion rate must be near to linearity [21].

The extrusion experiments were done at a temperature of 19–20 °C and changing rate from 10 to 60 rpm, by increasing by 10 rpm rate. Fig. 7 shows the relationship between extrusion pressure and rate is close to linearity. This show that mobility of the paste is good and higher the extrusion rate the green extrudate is more compact and homogeneous. Then, highest possible extrusion rate should be selected. However, surface defects were observed in the green extrudates produced at 50 and 60 rpm (Fig. 8). This type of surface defect, named "dog teeth", may occur along the structure as a result of excessive friction between the die and the material [21]. At lower extrusion rate no defects has been observed. Then, 40 rpm extrusion rate has been selected as the optimum conditions,

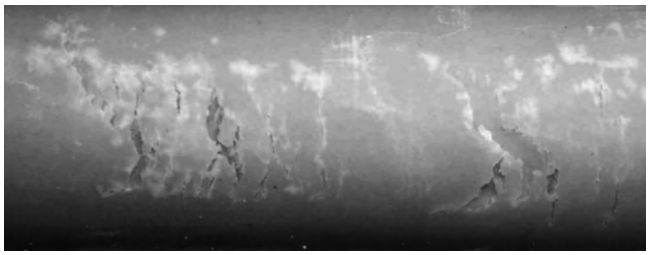

Fig. 8. "Dog teeth" type defects in the monolith extruded at a rate of 50 rpm.

as it led to a more compacted green extrudate without formation of defects.

Finally, to assess whether the extrusion process is good, it should be checked no water retention occurs during the process. Water retention occurs if water droplets appear in the mouth of the die [27], generally when the mixture has excess fluid. In that case the extrusion pressure is lower at high rate than at low rates [28]. This phenomenon was observed for none of the tests.

3.4. Optimization of the drying stage

Drying is the most difficult processes to optimize. The main difficulty in drying process is related with organic binder migration over the surface: As the water is evaporated from the surface, the binder remains in the body as waste; water is increasingly attracted to the surface to evaporate by the capillary forces, and it can carry binder leading to concentrate it on the surface. The main problems involved in migration of binder are: non-uniformity of binder concentration can led to weaker regions more sensible to the rupture; it also creates problems during firing due to the formation of a surface film [29].

The drying is generally carried out in four stages. In the first stage, the sample is heated to the drying temperature, so that surface water is evaporated and the sample is partially dried. Evaporation rate depends on raw materials, the texture of the sample and the chemical potential of water, related to the temperature and relative humidity in the atmosphere. Finally, the sample is completely dried by a combination of capillary flow and internal diffusion [30,31].

The drying of a ceramic body also involves shrinkage of the structure. If the shrinkage does not occur uniformly fracture and deformation can happen [32]. Typically, shrinkage of the structure occurs during the initial stages of drying as inter-particle water is evaporated. The temperature and humidity should therefore be carefully controlled so as to minimize the stress and distortion, and ultimately breakage [33,34].

Several tests were carried out by heating the green extrudates at different heating rates. Fig. 9 shows the type of fracture originated when a high heating rate is applied in the initial stage of the drying process: heating rate 0.5 °C min^{-1} from 20 °C and 80% RH to 110 °C and 0% RH This fracture occurs because the surface is dried faster than the inner zone leading to a non-uniform shrinking of the structure. Consequently central walls are separated one from the other originating longitudinal cracks in the structure. These cracks increase in width and length with temperature up to 60 °C; as temperature is increased its size was stabilized while the shrinking of the structure was more uniform.

Then, non-uniform shrinkage was avoided by lowering heating rate down to 0.15 °C min^{-1} at temperatures below 40 °C and keeping the relative humidity above 70%. In order to reduce drying time but avoiding formation of fractures, heating rate was increased as drying temperature was increased as shown in Table 4.

The monolith's shrinkage at the optimum conditions was 2.13%. Shrinkage can result in an enhancement of the mechanical strength,

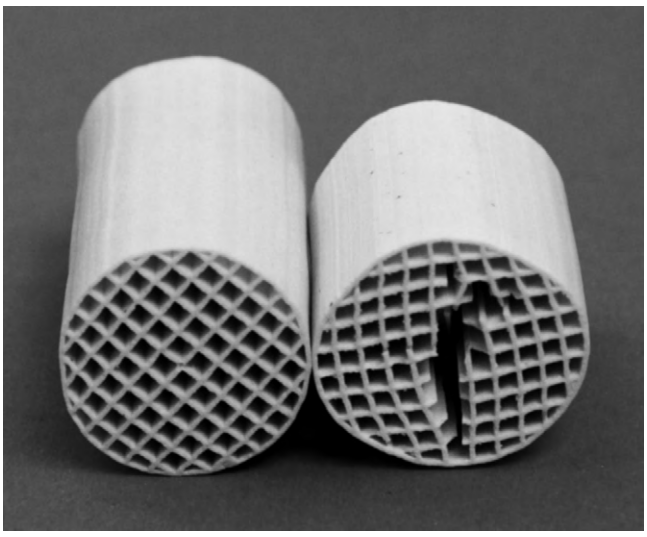

Fig. 9. Comparative image of two monoliths dried at different heating rate. (A) Heating conditions shown in Table 4; (B) heating rate 0.5 °C min^{-1} from 20 °C and 80% RH to 110 °C and 0% RH.

which is related to non-intracrystalline bond breakage between clay materials and non-plastic materials [35], but in this particular case a significant increase of mechanical strength is not expected. The acquisition of resistance allows handling without risk of breakage or deformation so that the cutting operation can be carried out without suffering damage.

3.5. Optimization of firing stage

The preparation of a zeolite monolith concludes with a firing step in order is to stabilize the chemical composition in the reactions conditions the catalyst will be used. Although applications for purifying off-gases are varied, most of them require temperatures up to 200–600 °C. Under these temperature conditions, binders and even zeolite can suffer chemical transformations that can affect to the physical and chemical properties of the catalytic monoliths, which can led to deformation and cracking of the monolith. Then, it was necessary to determine by trial and error, aided by the use of thermogravimetric analysis, the optimum temperature programme for the furnace.

In particular, the methylcellulose, being organic polymer is easily degraded above 225 °C [36] especially in oxidizing atmospheres. Fig. 10 shows the evolution of the mass of methylcellulose between 25 and 600 °C in a thermogravimetric analysis in an oxidizing atmosphere. Complete oxidation occurs at 500 °C.

The silica, used as permanent binder also suffers from transformation in its crystalline structure: quartz (up to 870 °C), tridymite (between 870 and 1470 °C) cristobalite (1470 and 1710 °C) and fused silica (>1710 °C). Although the four allotropic forms show a similar hardness, quartz is something harder.

The crystalline structure of the zeolite also undergoes changes at high temperature treatments, which may affect their catalytic properties. Table 5 shows the surface properties, such us surface

Table 4
Optimized drying conditions.

	Initial conditions	Final conditions	Heating rate
Stage 1	20 °C and 80% RH	40 °C and 70% RH	0.15 °C min^{-1}
Stage 2	40 °C and 70% RH	60 °C and 50% RH	0.5 °C min^{-1}
Stage 3	60 °C and 50% RH	100 °C and 0% RH	2.0 °C min^{-1}
Stage 4	110 °C	110 °C	120 min

RH: relative humidity.

Table 5
Surface properties of calcined H-ZSM-5 zeolite.

Calcining temperature, °C	S_{BET}, $m^2\ g^{-1}$	V_{micro}, $cm^3\ g^{-1}$	V_{meso}, $cm^3\ g^{-1}$	Total acidity, mmol $NH_3\ g^{-1}$	Weak acidity, mmol $NH_3\ g^{-1}$	Strong acidity, mmol $NH_3\ g^{-1}$
550	411	0.17	0.08	0.439	0.227	0.212
650	396	0.11	0.12	0.366	0.195	0.171
750	136	0.03	0.07	0.238	0.154	0.084

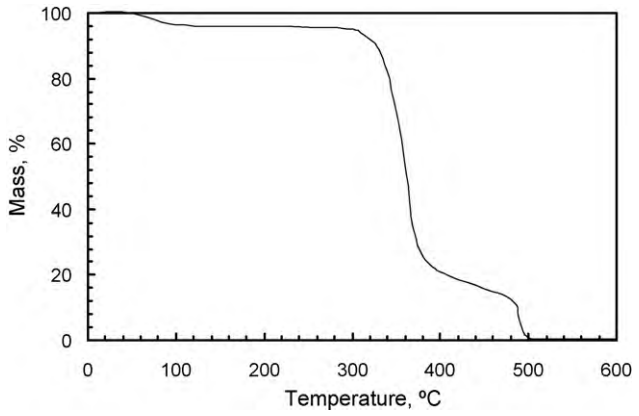

Fig. 10. Thermogravimetric analysis of methylcellulose.

Table 6
Optimized calcining conditions.

	Initial temperature, °C	Final temperature, °C	Heating rate/time
1st stage	20	120	1.0 °C min^{-1}
2nd stage	120	120	30 min
3rd stage	120	400	1.0 °C min^{-1}
4th stage	400	400	30 min
5th stage	400	600	10 °C min^{-1}
6th stage	600	600	30 min

area, pore volume and acidity of zeolite H-ZSM-5 calcined at different temperatures. The surface area and pore volume decreased significantly in more than 67% above 750 °C. The strong acidity decreases by 19% at 650 °C and by 60% at 750 °C compared to 550 °C.

According to the analysis of chemical stability of each component of the monolith showed above, firing temperature of 550 °C was chosen as the optimal value, since complete oxidation of methylcellulose polymer is achieved and catalytic properties of the zeolite are best maintained.

Another important variable is the heating rate, as the gas pressure generated in the oxidation of methylcellulose can cause bubbles in the structure, leading to surface defects that reduce the mechanical strength of the final monoliths. It was observed that heating rate higher than 1 °C min^{-1}, especially between 200 and 400 °C led to crack the monoliths due to the massive gas production during the polymer degradation (Fig. 10).

The optimized firing programme (Table 6) was divided in six segments. The objective of the first ramp segment 20–120 °C was to expel water absorbed by the zeolite (highly hydrophilic) between drying and firing process. The heating rate (1 °C min^{-1}) was considerably higher than the one used in the drying step because the low water content in comparison with the green monolith. A dwell segment of 30 min at 120 °C was added to assure complete removal of water. Then the temperature was raised to 400 °C at 1 °C/min followed by a second dwell segment (30 min) so that methylcellulose binder was burned off progressively. Ramp segment 3 (400–550 °C at 10 °C min^{-1}) and dwell segment 3 (30 min) were used to burn off all the organic contents. With this firing programme no physical and chemical defects were created during thermal processing.

During firing, monolith did not suffer further shrinkage. Then, resulted monolith's final density was 128 cell/in.^{2}.

Table 8
Characteristics of final monolith used for reaction.

Cell density	128 cpsi
Cell size	1.96 mm
Wall thickness	0.59 mm
Open-front area	76.2%
Diameter	23 mm
Length	21.8 mm
Geometric surface	1555 $m^2\ m^{-3}$
Specific surface (BET)	384 $m^2\ g^{-1}$
Monolith mass	3.38 g

3.6. Chemical and physical characterization of the zeolitic monoliths

Since the zeolitic monoliths will be used as catalysts in industrial reactors, most relevant physical and chemical properties of a catalyst were analyzed and compared with the raw zeolite.

Crystallinity of zeolites, determined by X-ray diffraction (XRD), remained unchanged after extrusion process. However BET surface area was reduced 9% with respect to the powder zeolite, although the pore volume has suffered a minor fall (Table 7). This reduction in BET surface may be due to plugging of some pores by the permanent binder SiO_2. Also acidity of the H-ZSM5 monolith was decreased by 57%, which may reduce its catalytic activity. The scanning electron microscopy (SEM) image of the zeolite powder (Fig. 11A) shows that the nano-crystals tend to form clusters with sizes of 0.25–0.5 μm. Unfortunately the size of the silica binder particles is too small to distinguish among the zeolite particles in the monolith by SEM (Fig. 11B). But the size of zeolite clusters in the monolith is more homogeneous and slightly higher, which can be interpreted as zeolite clusters being surrounded by silica particles or some zeolite clusters being joint each other (Fig. 11C).

The compressive crushing strength measured over 21 mm × 21 mm cylindrical probes according to ASTM C133-97 standard, showed a compressive ultimate stress of 2.58 ± 0.5 MPa.

The catalytic activity of catalysts was compared by monitoring the evolution of conversion with temperature, namely, the light-off curve [37]. Fig. 12 shows the light-off curves for DCE oxidation over raw zeolites in a fixed bed and the newly developed monolith (128 cells/in.^{2}). Table 8 summarizes the characteristics

Table 7
Comparison of BET and acidity between shaped monolith and raw H-ZSM-5 powder.

Sample	S_{BET}, $m^2\ g^{-1}$	V_{micro}, $cm^3\ g^{-1}$	V_{meso}, $cm^3\ g^{-1}$	Total acidity, mmol $NH_3\ g^{-1}$	Weak acidity, mmol $NH_3\ g^{-1}$	Strong acidity, mmol $NH_3\ g^{-1}$
H-ZSM-5 powder	411	0.17	0.08	0.286	0.103	0.183
H-ZSM-5 monolith	374	0.15	0.12	0.189	0.095	0.095

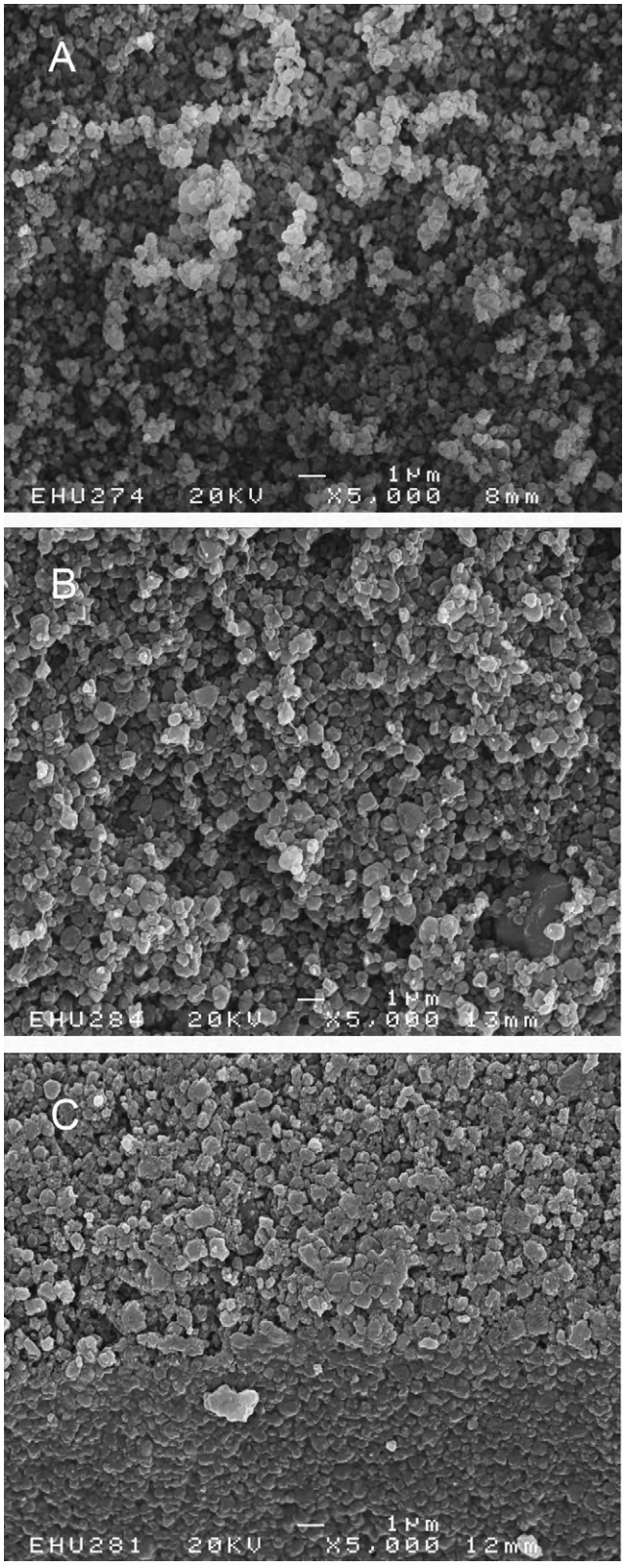

Fig. 11. Scanning electron micrograph of ZSM-5 zeolite: (A) commercial powder, (B) monolith: perpendicular cut to the monolith axis and (C) monolith: parallel cut to the monolith axis.

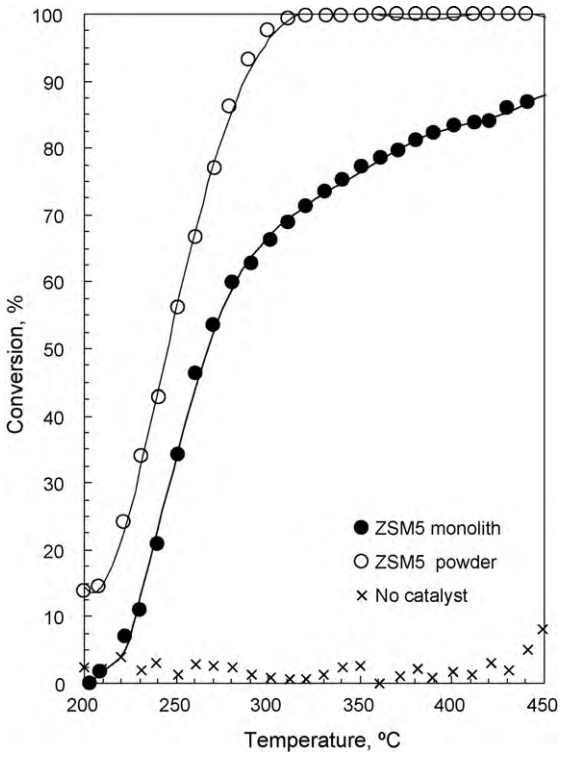

Fig. 12. Light-off curves of DCE oxidation over zeolitic monolith and raw zeolite powder (space velocity: 1.77×10^{-4} mol DCE kg^{-1} s^{-1}).

of the monolith. The new zeolitic monolith showed high activity in the oxidation of DCE, especially compared with oxidation in the absence of catalyst, in which, the conversion of DCE does not exceed 10% conversion in the temperature range evaluated; but activity is lower than the pure zeolite powder placed as a fixed bed. Recorded T_{50} (temperature to reach 50% conversion) values are: 245 °C for H-ZSM-5 as fixed bed and 270 °C for H-ZSM-5 as monolith. When comparing T_{90} (temperature to reach 90% of conversion), the differences are larger: 285 °C for H-ZSM-5 pure and > 450 °C for ZSM-5 monolith.

The decrease in activity of monolithic catalysts is due to two reasons. The first reason is the reduction of surface properties, such as the pore volume and the number of acid centres, due to the addition of permanent binder. This observation agrees with our previous investigations [38] and with those published in the literature [39]. At temperatures of low conversion (<250 °C), where reaction rate is proportional to conversion, the reaction rate in the monolith catalyst is about 53–60% lower than using pure zeolite powders. As reported above, acidity is reduced in the same proportions. Then, it reveals that acidity plays a key role in determining the activity of acidic catalysts since the oxidation of chlorinated hydrocarbons is initiated by the adsorption of the hydrocarbons on these sites.

The second reason is the difference in contact type between the reactants and the catalyst powder on a fixed bed catalytic reactor and on a monolith reactor. Although same mass of catalyst was placed in both type of reactor, the contact in a fixed bed reactor is superior to the contact in a monolith reactor. In the latter, it is common the overall chemical process to be controlled by mass-transport processes, generally slower than intrinsic catalytic reaction step. As the catalyst is deposited on the wall of the monolith channel, the reactant in the fluid phase has to be transported to the surface of the catalyst and within the catalyst. This transport happens by diffusion, while transport in the axial direction mainly happens by convection. Most gas phase reactions applied in monolithic reactors are relatively fast reactions (catalytic combustions,

oxidation reactions, etc.). Therefore, mass transfer from channel to the surface of the monolith wall by molecular diffusion is essential, which could affect the reaction process under certain operating conditions and monolith configurations [40,41]. As reaction rate is increased exponentially with the temperature, at high reaction temperatures diffusion of the reactants can be the rate-controlling step, leading slower increase of conversion with temperature in the light off curve (Fig. 12), and then higher T_{90}. Similar leveling-off in the conversion–temperature curves at conversions well below 100% can be observed in other works dealing with VOC combustion on monolith catalysts: e.g. Pina et al. [42] and Mazzarino and Barresi [43].

4. Conclusions

The manufacture of zeolites using the technique of direct extrusion of a zeolitic ceramic paste is based on a sequence of several processes (kneading, extruding, drying, firing) which are controlled by one or more variables. The aim of this work was to find out the operating conditions that led monolith of best quality.

It was found that good rheological properties to ensure successful extrusion though honeycomb shape die, depends on the paste composition and kneading temperature. By the addition of water quick increase of the drive torque was observed, followed by gradual decrease until stationary value was reached. It was found the stationary value of torque determine the quality of the paste. Below it, paste is easily deformable but it can collapse, while above it paste is cohesive but poorly deformable. Kneading temperature has also to be controlled and kept below 20 °C to avoid partial evaporation of water.

It was found that drying stage requires a strict control of heating rate and humidity to prevent the formation of fractures in the walls of the extrudate. Heating rates lower than 0.15 °C min^{-1} in the initial stages of drying prevents from the migration of the binder and led to a uniform shrinkage avoiding formation of fractures or deformities. The heating rate in the firing step must be lower than 1 °C min^{-1}, especially between 200 and 400 °C to prevent from cracking the monolith due to the massive gas production during the methylcellulose polymer degradation.

Acknowledgements

The authors wish to thank to the Spanish Education and Science Ministry (Project CTQ2008-03551) for the financial support. One of the authors (M.R.S.) acknowledges also to the Spanish Education and Science Ministry for the grant BES-2006-13729. The authors also kindly acknowledge the help of Professor Agustín Martínez Feliu from the Instituto de Tecnología Química, UPV-CSIC, in interpreting the SEM images.

References

[1] S.C. Larsen, in: V.H. Grassian (Ed.), Environmental Catalysis, Taylor and Francis Group, CRC Press, 2005, pp. 269–285.
[2] S. Irandoust, B. Andersson, Catal. Rev. Sci. Eng. 30 (1988) 341–392.
[3] G.B. Barannik, React. Kinet. Catal. Lett. 60 (1997) 291–296.
[4] P. Forzatti, D. Ballardini, L. Sighicelli, Catal. Today 41 (1998) 87–94.
[5] T.A. Nijhuis, A.E.W. Beers, T. Vergunst, I. Hoek, F. Kapteijn, J.A. Moulijn, Catal. Rev. Sci. Eng. 43 (2001) 345–380.
[6] J.L. Williams, Catal. Today 69 (2001) 3–9.
[7] P. Avila, M. Montes, E. Miro, Chem. Eng. J. 109 (2005) 11–36.
[8] A. Cybulski, J.A. Moulijn, Catal. Rev. Sci. Eng. 36 (1994) 179–270.
[9] J. Caro, M. Noack, P. Kölsch, R. Schäfer, Microporous Mesoporous Mater. 38 (2000) 3–24.
[10] L. Li, B. Xue, J. Chen, N. Guan, F. Zhang, D. Liu, H. Feng, Appl. Catal. A 292 (2005) 312–321.
[11] A. Bueno-Lopez, D. Lozano-Castello, I. Such-Basanez, J.M. Garcia-Cortes, M.J. Illan-Gomez, C. Salinas-Martinez de Lecea, Appl. Catal. B 58 (2005) 1–7.
[12] C.A. Grande, S. Cavenati, P. Barcia, J. Hammer, H.G. Fritz, A.E. Rodrigues, Chem. Eng. Sci. 61 (2006) 3053–3067.
[13] Y.Y. Li, S.P. Perera, B.D. Crittenden, Trans. IChemE 76 (1998) 921–930.
[14] Y.Y. Li, S.P. Perera, B.D. Crittenden, J. Bridgwater, Powder Technol. 116 (2001) 85–96.
[15] K. Shams, S.J. Mirmohammadi, Microporous Mesoporous Mater. 106 (2007) 268–277.
[16] J. Benbow, J. Bridgwater, Paste Flow and Extrusion, Clarendon Press, Oxford, 1993.
[17] A. Aranzabal, J.A. González-Marcos, M. Romero-Sáez, J.R. González-Velasco, M. Guillemot, P. Magnnoux, Appl. Catal. B 88 (2009) 533–541.
[18] I. Nieto, Fabricación de Monolitos de Base Zeolítica de Aplicabilidad Industrial Empleando como Aglomerantes Resinas de Silicona, M.S. Thesis, University of the Basque Country, Dpt. of Chemical Engineering, 2003.
[19] M. Okuyama, T. Fukui, C. Sakurai, J. Non-Cryst. Solids 144 (1992) 298–304.
[20] G.W. Phelps, M.G. McLaren, in: G.Y. Onoda Jr., L.L. Hench (Eds.), Ceramic Processing Before Firing, Wiley-Interscience Publication, Florida, 1978, pp. 211–225.
[21] G.C. Robinson, in: G.Y. Onoda Jr., L.L. Hench (Eds.), Ceramic Processing Before Firing, Wiley-Interscience Publication, Florida, 1978, pp. 391–407.
[22] R. Ferret, Synthesis of cordierite by solid-state reaction and optimization of the extrusion process of monolith structures, PhD Thesis, Bilbao, 2000.
[23] D. Ballardini, L. Sighicelli, C. Orsenigo, L. Visconti, E. Tronconi, P. Forzatti, A. Bahamonde, E. Atanes, J.P. Gomez Martin, F. Bregani, Stud. Surf. Sci. Catal. 101 (1996) 1359–1368.
[24] H. Bohm, S. Blackburn, Br. Ceram. Trans. 5 (1994) 169–177.
[25] J.J. Benbow, S.H. Jazayeri, J. Bridgwater, Ceram. Trans. 1 (1988) 624–634.
[26] G.Y. Onoda Jr., in: G.Y. Onoda Jr., L.L. Hench (Eds.), Ceramic Processing Before Firing, Wiley-Interscience Publication, Florida, 1978, pp. 235–252.
[27] C. Treischel, E.W. Emrich, J. Am. Ceram. Soc. 29 (1946) 129–132.
[28] J. Benbow, S.H. Jazayeri, J. Bridgwater Ceram. Trans. 1 (1988) 624–634.
[29] G.K. Sarkar Jr., Greminger Ceram. Bull. 62 (1983) 1280–1284.
[30] Liptak, Chem. Eng. 2 (1998) 110–114.
[31] J.M.F. Blanchart, Weber, J. Mater. Sci. 30 (1995) 2319–2324.
[32] Cooper, in: G.Y. Onoda Jr., L.L. Hench (Eds.), Ceramic Processing Before Firing, Wiley-Interscience Publication, Florida, 1978, pp. 261–276.
[33] M. Sheppard, Ceram. Bull. 68 (1989) 1815–1820.
[34] R. Herman, Ceramic Monographs-Handbook of Ceramics, Monograph 1.5.3, vol. 38, 1989.
[35] W.O. Williamson, in: G.Y. Onoda Jr., L.L. Hench (Eds.), Ceramic Processing Before Firing, Wiley-Interscience Publication, Florida, 1978, pp. 377–389.
[36] J.E. Schuetz, Ceram. Bull. 65 (1986) 1556–1559.
[37] F. Duprant, Chem. Eng. Sci. 57 (2002) 901–911.
[38] R. López-Fonseca, B. de Rivas, J.I. Gutiérrez-Ortiz, A. Aranzabal, J.R. González-Velasco, Appl. Catal. B 41 (2003) 31–42.
[39] T.E. McMinn, F.C. Moates, J.T. Richardson, Appl. Catal. B 31 (2001) 93–105.
[40] K. Ramanathana, V. Balakotaiaha, D.H. Westb, Chem. Eng. Sci. 58 (2003) 1381–1405.
[41] J. Chena, H. Yanga, N. Wanga, Z. Ringa, T. Dabrosb, Appl. Catal. A 31 (2008) 1–11.
[42] M.P. Pina, S. Irusta, M. Menéndez, J. Santamaría, R. Hughes, N. Boag, Ind. Eng. Chem. Res. 36 (1997) 4557–4566.
[43] I. Mazzarino, A.A. Barresi, Catal. Today 17 (1993) 335–347.